Spectrochimica Acta Part A: Molecular and Biomolecular Spectroscopy 244 (2021) 118895

Contents lists available at ScienceDirect

Spectrochimica Acta Part A: Molecular and Biomolecular Spectroscopy

journal homepage: www.elsevier.com/locate/saa

Short Communication

Determination of vibrational band positions in the E-hook of β-tubulin

Ashley E. Williams [a], Juliana E. Davis [b,1], Justin E. Reynolds [b,1], Ryan C. Fortenberry [a], Nathan I. Hammer [a], Dana N. Reinemann [b,c,*]

[a] Department of Chemistry and Biochemistry, University of Mississippi, University, MS 38677, United States of America
[b] Department of Biomedical Engineering, University of Mississippi, University, MS 38677, United States of America
[c] Department of Chemical Engineering, University of Mississippi, University, MS 38677, United States of America

ARTICLE INFO

Article history:
Received 15 January 2020
Received in revised form 22 May 2020
Accepted 25 August 2020
Available online 28 August 2020

ABSTRACT

Raman spectral characterization of the β-TUBB2A E-hook hexapeptide, EGEDEA, is determined through experimental analysis combined with full geometry optimizations and corresponding harmonic vibrational frequency computations employing DFT methods. The hexapeptide is first broken down into di- and tetrapeptide fragments which are analyzed both quantum chemically and experimentally, and then combined to achieve an energetic minimum of the large EGEDEA hexapeptide. The Raman spectral characterization of EGEDEA band positions are then verified via the literature and comparison to the small fragment's similarly located band positions. The approach employed provides further evidence for the use of fragments as a helpful tool in characterization of the vibrational band positions of large peptides.

Statement of significance: To investigate β-TUBB2A E-hook hexapeptide, a unique approach is employed whereby the hexapeptide is broken into fragments, EG, ED, EA, EGED, and EDEA and analyzed via experimental Raman spectroscopy of the crystalline solids. The experimentally observed vibrational band positions are compared to those computed using and scaled from DFT methods and Pople's 6-311+G(2*df*,2*pd*) basis set. The reported vibrational band positions are also confirmed by previously reported bands of similar peptides in the literature. This methodology facilitates differentiation between the behaviors of various side chains and their influence on the structure of the hexapeptide, providing insight into not only the nature of the peptide but also defining regions for potential protein and cytoplasmic interactions, without requiring excessive computing resources or overly-sensitive experimental methods.

1. Introduction

Microtubules (MTs) are pervasive throughout cells and serve as structural filaments, enable dynamic machinery, such as the mitotic spindle, and act as tracks for molecular motor proteins [2–5]. MTs consist of α- and β-tubulin dimers and contain disordered, C-terminal tails, known as E-hooks, which extend from the MT surface to interact with the cytoplasmic environment [7,8]. While the MT core is conserved, the highly negatively charged E-hook composition differs depending on its location and proposed function [8–13]. The presence and upregulation of βIII E-hooks have been correlated with tumor development, cancer aggressiveness, and resistance to MT-based chemotherapies [9,13–15]. E-hooks also engage in the binding and processive motility of kinesin and dynein molecular motors [8,10,16–19]. These motor proteins "walk" along MTs through conformational changes via ATP hydrolysis to perform essential tasks such as directed cargo transport [4,8–10,17,20–24].

Despite the E-hook's clear importance in cytoskeletal regulation and function, its molecular structure is not well understood. Structural characterization and manipulation methods have been used to investigate tubulin and its interaction with motor proteins, but the E-hook structure alone remains elusive. Crystallography has produced high-resolution structures of the tubulin core but has been unable to resolve the disordered E-hook tail [26–28]. In addition, NMR and single molecule methods have characterized and evaluated the effect of E-hook mutations on cell function [9,27–29]. Molecular dynamics simulations have scored E-hook interactions with tubulin or microtubule associated proteins (MAPs) [11,26,30,31], but physiological environmental influences on its structure are not well known.

Raman spectroscopy, surface enhanced Raman spectroscopy (SERS), and quantum chemical approximations in both the solid state and solution have been essential tools in investigating amino acid molecular structure through vibrational analysis [1,6,25,32–38]. Raman spectroscopy is insensitive to water and thus its use in studying biological molecules in aqueous environments provides information that other

* Corresponding author at: Department of Biomedical Engineering, University of Mississippi, University, MS 38677, United States of America.
E-mail address: dnreinem@olemiss.edu (D.N. Reinemann).
[1] Contributed equally.

https://doi.org/10.1016/j.saa.2020.118895
1386-1425/

methods commonly used in investigation of molecular structure (FTIR, X-ray diffraction, NMR) cannot. Most notably, Raman spectroscopy details environmental effects and can predict and capture the effects of inter-and intramolecular hydrogen bonding on molecular structure and molecular vibrations. Furthermore, Raman spectroscopy requires little to no sample preparation and is not destructive to the material under study. Thus, such a spectroscopic approach preserves the biological activity of the molecule and allows investigation of conformational changes to occur in real time and *in vivo* [40]. Several reference databases of biological molecules, including the amino acids glycine, L-alanine, and L-glutamic acid, compare the Raman spectra of the individual amino acids to the Raman spectra of larger biomolecules such as cellulose, acetyl coenzyme A, and riboflavin [41]. Larger peptide fragments have been investigated with DFT analysis compared to experimental vibrational spectra to elucidate the molecular vibrations and implications of solvation on molecular structure, including isolated amino acid residues [6,25,34–37,42–44], dipeptides [39,45–53], tripeptides [54–60], and larger peptide fragments [17,48,61–65]. SERS employed on small peptide fragments and proteins has also achieved the signal necessary to assign band positions of large molecules [67–72].

Previous studies of Raman spectra of short peptide fragments compare well with separate spectra of large proteins, providing insight into the molecular conformation and topology of more complex molecules [1,33,39,52,59]. Kausar and co-workers reported Raman spectra of both the solid state and aqueous solution of the dipeptide L-aspartyl-L-glutamic acid (DE) [39]. Elstner *et al.* quantum chemically computed the geometries and relative energies of small glycine and alanine based polypeptides containing up to eight residues via density function theory (DFT) [33]. This and other studies reveal that comparison of experimental Raman vibrational modes to DFT-predicted modes agree well and have successfully described the vibrational motions of the investigated biomolecules [25,39,49,51,55,59,73,74]. Sjöberg and coworkers reported the experimental Raman band positions of tripeptides with the basic formula GlyAAGly where the central amino acid (AA) varied. B3LYP/6-311+G(2*df*,2*pd*) band positions of the amino acid side chains tracked well with experiments and showed that the band positions of the side chains blue shift in the tripeptides compared to the free amino acids [59].

β-TUBB2A tubulin's C-terminal tail, or E-hook, is composed of the amino acid residues EGEDEA at its periphery. The hexapeptide is analyzed here using Raman spectroscopy in conjunction with electronic structure computations and the literature via a stepwise build-up mechanism. This approach allows for the utmost control over the interpretation of the peptide's vibrational modes. E-hooks are usually 10–18 residues in length, and the last six residues, EGEDEA [13,18], are highly electronegative and directly interact with proteins and the environment. The last six residues of the β-TUBB2A E-hook are used as a representative peptide due to its overall negative charge, and a shorter peptide is more manageable to analyze spectroscopically and quantum chemically. Description of the vibrational band positions in a complex peptide first requires breaking the peptide into small fragments and then performing vibrational analysis on those, as described in the literature [50,55,64]. The spectroscopic patterns revealed in the fragments can then be used to assign the intense vibrational positions in the larger peptide with greater accuracy [50]. Furthermore, peptide fragments have been employed to describe structural insight and characterize vibrational motions, such as the secondary structures of large peptides, obtained from a variety of different techniques (SERS, FTIR, Raman, Vibrational Circular Dichroism, ssNMR) and have proven to provide accurate representations of the parent peptide [1,44,46,50,55,59,62,64,75]. Thus, the 6-amino acid EGEDEA peptide is broken into small fragments, EG, ED, EA, EGED, and EDEA, and analyzed both experimentally and via DFT (density functional theory) and WFT (wave function theory) analysis. The fragments are then compared to experimental and quantum chemical analysis of the full EGEDEA hexapeptide to validate that the build-up approach accurately describes the full peptide spectrum. This methodology facilitates differentiation between the behaviors of various side chains, providing insight into not only the nature of the peptide but also aids in elucidating the driving forces for protein and cytoplasmic interactions with the E-hook.

2. Methods

2.1. Materials

The β-TUBB2A E-hook in the form of a synthetic peptide of charged amino acid sequence $EGEDEA^{4-}$ is acquired in crystalline form from Genscript at >95% purity. Additional peptide fragments EG^{1-}, ED^{2-}, EA^{1-}, $EGED^{3-}$, and $EDEA^{3-}$ are also acquired in the same manner and purity. The samples are stored at −20 °C to maintain their integrity for experimental Raman analysis.

2.2. Experimental methods

A Horiba Scientific LabRAM HR Evolution Raman Spectroscopy system with CCD camera detection is used to analyze the crystal solids of the peptide fragments. Raman spectroscopy is preferable to infrared absorption spectroscopy because of the favorable relative Raman activities of water to biopolymers. A 532 nm laser line is used as the excitation source, and either a 600 or 1800 grooves/mm grating is used for detection, affording a resolution of less than 1 cm^{-1}. The instrument allows for the characterization of the effects of the environment through analysis of vibrational spectroscopic shifts. Additionally, Raman studies at −100 °C utilize a temperature-controlled stage allowing formation of crystals via controlled flow of liquid nitrogen over the sample. The vibrational characterization of only the EGEDEA hexapeptide is performed with the temperature-controlled data acquired.

2.3. Theoretical methods

All computations are performed using the Gaussian16 software program [76]. Full geometry optimizations and harmonic vibrational frequency computations determine a structural local minimum of the peptide and the corresponding vibrational frequencies and Raman activities of the normal modes. Finding the global minimum of the 77 atom hexapeptide is computationally unapproachable; thus, our approach breaks the polypeptide into manageable fragments and tracks how the band positions and Raman activities evolve with increasing basis set size. Molecular dynamics simulations are commonly employed to investigate the interactions of large proteins in different solvation shells. However, recently, more accurate quantum chemical methods have facilitated more detailed analysis of peptide molecular structure [9,23,29–31]. Investigation of the quantum chemically approximated vibrational frequencies of increasingly large systems at higher levels of theory is an evolving frontier [9,23,29–31].

A low-energy local minima for the EGEDEA hexapeptide is produced by breaking down the peptide into three amino acid dipeptide fragments, EG, ED, and EA and optimizing them using the B3LYP method with increasing basis sets: 3-21G, 6-31G, 6-31+G(*d*,*p*), and 6-311+G(2*df*,2*pd*) [77–79]. The B3LYP/6-311+G(2*df*,2*pd*) level of theory has been used in the literature to describe smaller biological peptides [25,39,59,73]. Diffuse hydrogen orbitals are also included because the peptide is an anion with an overall −4 charge necessitating their inclusion. Harmonic vibrational frequency computations are undertaken at each of the aforementioned levels of theory. The optimized dipeptides are then coupled into two different tetrapeptides, EGED and EDEA and the minimum-energy structures are again obtained using the same method described above. The accuracy of the vibrational band positions in comparison to the EGEDEA Raman experimental bands is validated by optimizing the hexapeptide with a guess conformation determined from the tetrapeptides coupled to form the hexapeptide structure at the B3LYP method and 3-21G, 6-31G, 6-31+G(*d*,*p*), and 6-311+G

(2*df*,2*pd*) basis sets. There are various φ and ψ rotations large peptide sequences can explore, but this step-wise analysis promotes accurate characterization of rotation about the peptide bond without doing a full potential energy rotamer scan, as demonstrated by comparing Raman spectra in the Results and Discussion.

Simulated Raman spectra are created by summing Lorentzian profiles for each calculated normal mode and weighting with the corresponding Raman activity. A scaling factor of 0.97 is used for all levels of theory to partially account for the anharmonicity of the computed harmonic vibrations. This value has been previously reported to correct the overestimation of the vibrational frequencies acquired using B3LYP/6-311+G(2*df*,2*pd*) [80].

Performing a total energy distribution (TED) on molecules of this size is nearly impossible, thus determination of which atomic motions are part of the vibrational frequencies is performed qualitatively by visually determining which atomic motions are most intense for each vibrational frequency. Analysis of the vectors of the atomic motions for each vibration is interpreted as we have qualitatively defined them. Throughout the characterization of each peptide fragment, all of the atomic motions are described in the "Assignment" column, with the greatest contribution (most intense displacement) represented in bolded text (ESI, Tables S1–S6).

3. Results and discussion

Here, the vibrational band positions of the E-hook's C-terminal sequence are characterized through coupling analysis of experimental spectra and computationally predicted vibrations. The representative amino acid sequence EGEDEA is broken down into component dipeptides EG, ED, and EA for analysis via experimental Raman spectroscopy and with the B3LYP/6-311+G(2*df*,2*pd*) level of theory (Fig. 1). The dipeptides are then coupled computationally to form tetrapeptides EGED and EDEA, and finally the tetrapeptides into the final EGEDEA hexapeptide, and compared to experimental spectra for each fragment. The experimental Raman spectral signatures of E-hook di-, tetra-, and hexapeptide fragments, which consist of similar amino acids but varying in size and order, exhibit remarkable agreement with one another (Table 1, Fig. 2). The Raman vibrational modes of the E-hook hexapeptide are characterized from analysis of the smaller peptide fragments, clearly linking the atomic motions to the experimental modes (Table 1). The DFT band positions, in combination with previously reported band positions in the literature, characterize the peptide fragments studied here. One of the challenges of characterizing the vibrational modes of peptides is the large number of motions that can occur at each band position. Often, the stretching of one amino acid side chain results in full peptide bends and twists in response, as evidenced by visualizing the vibrations from our DFT calculations. The literature has worked around this issue by reporting all of the motions found at each band position; however, descriptions of these vibrations are open to interpretation without correlating to known atomic behavior such as that from smaller molecules incorporated into larger systems.

The agreement found among the experimental Raman spectra for each of the dipeptides, tetrapeptides, and hexapeptide indicates that small peptide fragments can be used to assign Raman bands in larger peptides (Fig. 2). The simulated spectrum for each fragment also agrees well with experiment, supporting its use to verify the vibrational motions occurring at each band (ESI, Figs. S1–S6, Tables S1–S6). Full vibrational analysis (as described in Section 2.3 Theoretical methods) was performed on each of the peptide fragments, and resulting data is included in the ESI (Tables S1–S6).

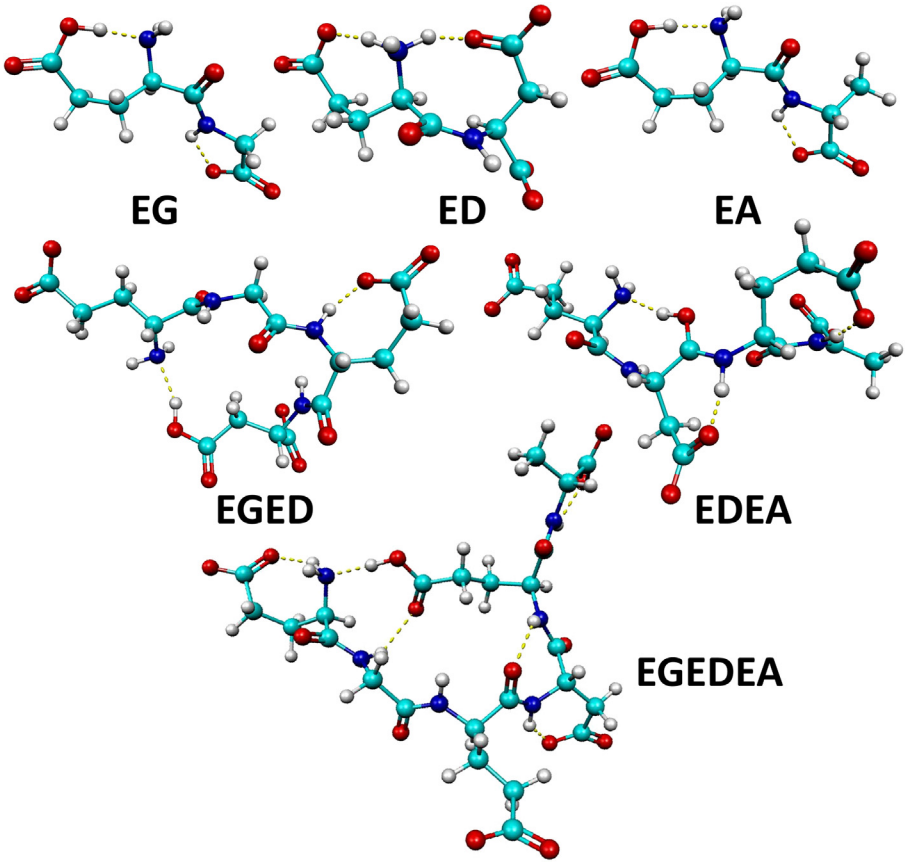

Fig. 1. Molecular geometries for the dipeptide fragments, EG, ED, and EA, tetrapeptide fragments, EGED and EDEA, and full hexapeptide, EGEDEA computed at the B3LYP/6-311+G(2*df*,2*pd*) level of theory. Dotted lines represent locations of intramolecular hydrogen bonding.

Table 1
Excerpt from the comparison of the experimental vibrational band positions corresponding to the same vibrational motions confirmed with harmonic frequency calculations for the EG, ED, and EA dipeptide fragments, EGED and EDEA tetrapeptide fragments, and the full EGEDEA hexapeptide. The assigned vibrational modes are compared to previously reported vibrational motions in the literature (Reference). Values are Raman Shift (cm^{-1}).

EG	ED	EA	EGED	EDEA	EGEDEA	Reference[a]	Assignment[b]
828	804	750	829	840	842	ν(C—N), ν(C—C) [1],δ(C-C-O) [1], ω(COO-) [6], Υ(NH) [25], $\delta(NH_2)$ [39]	$\rho(\alpha NH_3^+)$, E1 residue $\nu_s(\alpha N^*\text{-}\alpha C_{E1}\text{-}C)$, $\delta(\alpha N^*\text{-}\alpha C_{E1}\text{-}C)$, ν_s(C—C), v_{as}(C-C-cC), δ(O-cC=O)
1183	1207	1210	1196	1205	1209	$\Upsilon(CH_2)$ [25], $\tau(CH_2)$ [39], $\rho(CH_2)$ [6]	G residue $\nu_s(N\text{-}\alpha C_G\text{-}C(O)_2)$ & $\tau(CH_2)$, E2 residue ω(C—H) & $\rho(CH_2)$, ω(N—H)
1305	1300	1306	1313	1281	1314	$\tau(CH_2)$ [25,59,66], ν(C—N) [39], ν(C—C) [1,6], ν_s(COO-) [1], $\rho(CH_2)$ [6]	ν_s(O-αC*=O), A residue $\delta(CH_3)$ & $\omega(\alpha C_A\text{-}H)$,
1338	1322	1351	1328	1322	1327	ν(COO-), ν(N-C-H) [1], $\delta(CH_2)$ [6,35,39,59], $\omega(CH_2)$ [37,39,66], $\Upsilon(CH_2)$ [25]	E2 and D residue ν_s(O-cC=O), ω(αC-H), & $\rho(CH_2)$, A residue $\delta(CH_3)$ & $\omega(\alpha C_A\text{-}H)$
1448	1430	1438	1435	1442	1437	$\delta(CH_2)$ [6,25,35,39], $\Upsilon(CH_2)$ [37], σ (CH_2) [59,66]	E3 residue $\delta(CH_2)$ & A residue $\delta(CH_3)$
1518	1425	1462	1479	1482	1508	$\Upsilon(NH_2)$ [66]	Amide *I* ν(C—N), $\nu_s(O_3{=}C\text{-}N)$, & ω(N—H)
1648	1620	1651	1622	1678	1611	ν_{as}(COO-) [1,25,35,37,39,59,66]	Amide *V* ν(C=O_5), ν_{as}(O-αC*=O) & $\nu(\alpha C_A\text{-}\alpha C^*)$
1733	1700	1723	1686	1705	1679	$\nu(C{=}O)_{skel}$ [25,35,37,39,59], δ(H-O-H) [25], ν(C—N) [39], $\delta(NH_3)$ [59,66]	$\delta(\alpha NH_3^+)$, Amide *I* $\nu(C{=}O_1)$, $\nu_s(\alpha C_{E1}\text{-}C(O)_1\text{-}N)$, Amide II $\nu(C{=}O_2)$, $\nu_s(\alpha C_G\text{-}C(O)_2\text{-}N)$, E3 residue ν_{as}(O-cC=O) & protonated ω(O—H)
2917	2894	2920	2896	2882	2914	E residue $\nu(CH_2)$ [25], $\nu_s(CH_2)$ [37,39,66]	E1 residue $\nu_s(CH_2)$
3305	3371	3282	3367	3382	3174	ν_s(N—H) [25]	$\nu(\alpha N^*\text{-}H)$, $\nu_s(\alpha NH_3^+)$

Symbols: δ = Bending, ν = Stretching, τ = Twisting, ρ = Rocking, ω = Wagging, Υ = Deformation, σ = Scissoring, as = antisymmetric, s = symmetric, skel = full peptide, αN^* = α-Amino terminal N, αC^* = α-Carboxy terminal C.
[a] Previously assigned vibrational modes in other peptides with citations.
[b] Peptide vibrational modes assigned in this study.

Fig. 2 and Table 1 compare the experimental Raman spectra for solid EG, ED, and EA dipeptides, EGED and EDEA tetrapeptides, and EGEDEA hexapeptide. The full characterization table can be found in the ESI (Table S13). The most intense band in each spectrum corresponds to the E1 residue symmetric C—H stretching, $\nu_s(CH_2)$ (closest to the N terminus). This same band, corresponding to the same vibrational motion, is found to be the most intense band in nearly the same position in all of the peptide fragments under study. In the EGEDEA hexapeptide experimental Raman spectrum, this band appears at 2914 cm^{-1}. As the peptide fragment is decreased from six amino acids to four, this band red shifts to 2882 cm^{-1} (EDEA) and 2896 cm^{-1} (EGED). This red-shifting trend is again observed when decreasing the peptide fragment size to include the ED amino acids, with the band appearing at 2894 cm^{-1}. In the EG and EA spectra (Fig. 2), this band is actually blue-shifted from the original EGEDEA band at 2914 cm^{-1}, appearing at 2917 cm^{-1} (EG) and 2920 cm^{-1} (EA) [1,25,39]. This behavior can be explained by the nature of the amino acid side chains represented by each fragment. In the EG and EA dipeptides, the negatively charged glutamic acid residue is offset by a nonpolar glycine and alanine residue. There is a lesser extent of partial conjugation into the peptide bond due to the presence of only two carboxylic acids donating electron density into the partially conjugated backbone. The C-terminal carboxy group is offset by a

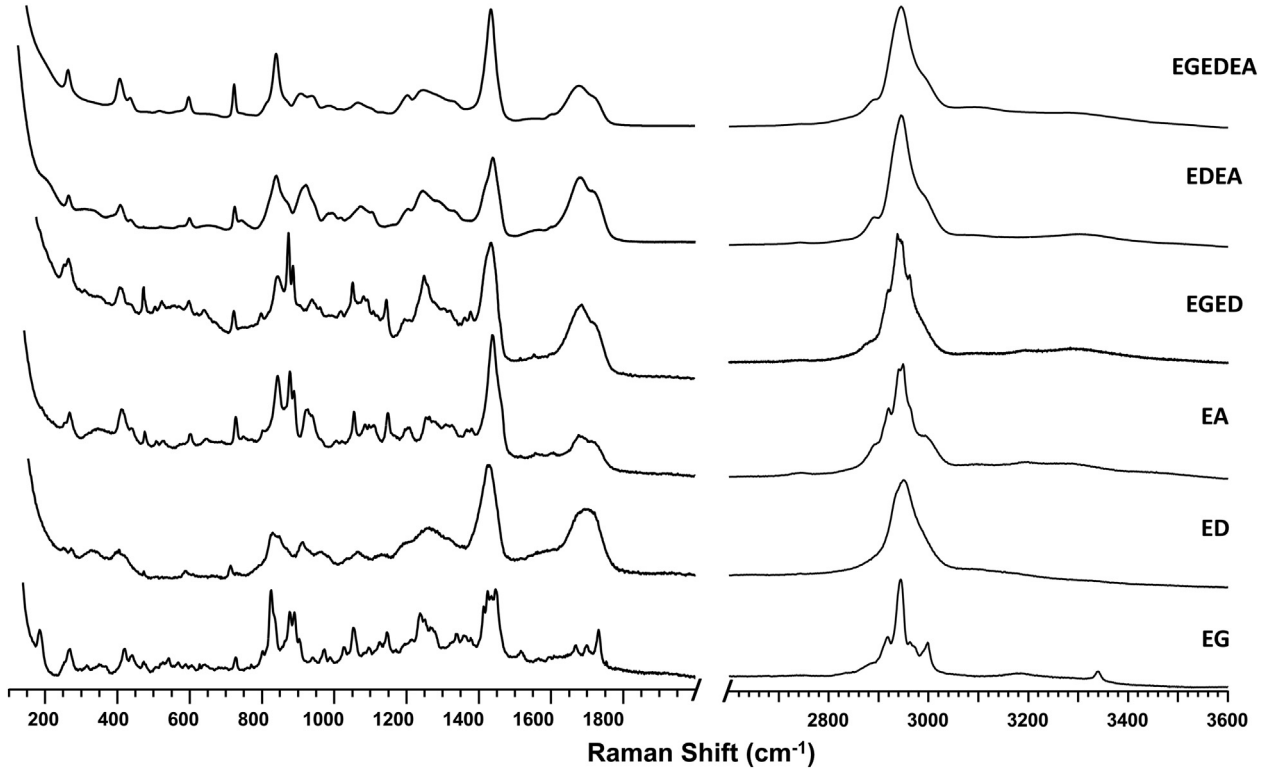

Fig. 2. Experimental Raman spectra for each of the dipeptide fragments (EG, ED, and EA) compared to the tetrapeptide fragments (EGED and EDEA) compared to the full hexapeptide, EGEDEA.

nonpolar glycine or alanine residue, resulting in a decrease in the magnitude of charge delocalization when compared to the fragments containing multiple neighboring charged amino acid side chains. This side-chain effect results in a decrease in energy of this vibrational band and corresponding red-shifted photons. When introducing a greater number of charged side chains, however, the presence of additional negative charge and corresponding electron density represented by the fragment results in a greater extent of partial conjugation and thus blue-shifted photons. This is apparent with the ED, EGED, and EDEA peptide fragments' (all of which contain neighboring negatively-charged amino acid side chains) bands blue-shifted to higher energy positions.

Another region of interest is ~1435 cm^{-1}. In the EGEDEA hexapeptide experimental Raman spectrum, this band appears at 1437 cm^{-1} and corresponds primarily to an H-C-H bending motion ($\delta(CH_2)$) in the E3 and A residues (closest to the C-terminal end of the fragment). This band appears in the EG dipeptide spectrum at 1448 cm^{-1}, the EA spectrum at 1438 cm^{-1}, and the ED spectrum at 1430 cm^{-1}. This band appears in the tetrapeptide fragments at 1435 cm^{-1} (EGED) and 1442 cm^{-1} (EDEA). In the EG, ED, and EGED spectra, this band is the E residue methyl bending motion, (E2 residue in EGED), $\delta(CH_2)$ [1,25,42,59]. Interestingly, in each of the peptide fragments that display the EA amino acids together (EA, EDEA, and EGEDEA), this band corresponds to a coupled motion, including both the E and A residue methyl bending vibrations $\delta(CH_2)$ and $\delta(CH_3)$ [35,37]. As the peptide fragment is increased from the dipeptide, EA, to the tetrapeptide, EDEA, this band is blue-shifted from 1438 cm^{-1} to 1442 cm^{-1}. The addition of the two negatively-charged side chains, E and D, to the dipeptide results in a greater extent of charge density delocalized into the conjugated peptide backbone, resulting in this band shifting to higher energy. Upon addition of the EG residues to the EDEA tetrapeptide, however, this band red-shifts to 1437 cm^{-1} which can be attributed to the nonpolar G residue side chain disrupting the delocalization into the backbone and resulting in red-shifted photons, or a shift to lower energy. In the peptide fragments containing neighboring charged amino acid side chains but lacking the A residue (ED: 1430 cm^{-1} and EGED: 1435 cm^{-1}), this band is red-shifted from the fragments containing both E and A residues. The motion corresponds to only the E residue methyl bending motion (E2 residue in the EGED tetrapeptide). Without the neighboring A residue, there is less disruption of the distribution of the E residue's negative electron density into the peptide backbone, resulting in shortening of the bonds and corresponding decrease in energy. The only exception is the EG dipeptide, in which the E residue's methyl bending vibration ($\delta(CH_2)$) is blue-shifted from all of the other bands, to 1448 cm^{-1}. Without the nonpolar A residue's $\delta(CH_3)$ motion and a neighboring D residue adding electron density into the molecule, the E residue's methyl bend $\delta(CH_2)$ results in lengthening of the bonds and a corresponding shift to a higher energy position.

Several of the peaks appear to be broadened in the larger peptide fragments, arising from a greater extent of intermolecular interactions and possibly disordering of the crystalline solids. The peak at ~1680 cm^{-1} (EG-1733 cm^{-1}; ED-1700 cm^{-1}; EA-1723 cm^{-1}; EGED-1686 cm^{-1}; EDEA-1705 cm^{-1}, EGEDEA-1679 cm^{-1}) generally corresponds to a backbone carbonyl stretching motion, $\nu(C{=}O)_{skel}$ [25,35,37,39,59], as well as bending of the charged N terminus, $\delta(NH_3^+)$. Despite the broadness of the peaks, there is close agreement between the EGED spectrum at 1686 cm^{-1}, the EDEA spectrum at 1705 cm^{-1}, and EGEDEA spectrum at 1679 cm^{-1}. In each of these band positions, the vibration primarily corresponds to the Amide *I* $\nu(C{=}O_1)$ stretch and $\delta(NH_3^+)$ bend. Together, the agreement confirms the location of this mode and demonstrates the advantage of using smaller peptide fragments to describe larger biomolecules.

There are a number of peaks present in the larger fragments that are not visible in the dipeptide spectra simply because there are a greater number of residues in the larger fragments. Additionally, many of the vibrational band positions in the larger fragments arise from coupling of motions that are not possible in the smaller fragments due to the lack of residues. There are three peptide bonds present in each of the tetrapeptide fragments and five peptide bonds present in the EGEDEA hexapeptide. The resolution provided by the Raman spectrometer employed allows for discernment of each of the amide stretching vibrational motions, ν(C—N). In the EGEDEA hexapeptide, the Amide I ν(C—N) motion appears at 1508 cm^{-1}, Amide II at 1494 cm^{-1}, Amide III at 1480 cm^{-1}, Amide IV at 1487 cm^{-1}, and Amide *V* coupled with both the Amide II and Amide IV stretches at 1494 and 1487 cm^{-1}. This is similarly observed in the tetrapeptide fragments. For example, in the EGED tetrapeptide, the Amide I stretching motion ν(C—N) appears at 1479 cm^{-1}, Amide II at 1533 cm^{-1}, and Amide III at 1490 cm^{-1}. Combined with DFT computations performed at the triple-ζ level of theory, these individual motions are isolated and confirmed, which is difficult for molecules of this magnitude. These results imply that such a buildup mechanism can clearly elucidate vibrational spectra and molecular structure without the need for over-complicated experimental techniques or molecular dynamics simulations.

CRediT authorship contribution statement

AEW was involved in all aspects of the work, including performing experiments, calculations, data analysis, and preparation of the manuscript. AEW, JED, JER, NIH, and DNR designed the research and performed data analysis. AEW, RCF, NIH, and DNR designed the computational work. AEW, JED, JER, RCF, NIH, and DNR prepared the manuscript.

Declaration of competing interest

The authors declare no conflicts of interest.

Acknowledgements

AEW and NIH are supported by the National Science Foundation (NSF) under grant number CHE-1532079. NIH and RCF are supported from NSF grant CHE-1757220.

Appendix A. Supplementary data

Supplementary data to this article can be found online at https://doi.org/10.1016/j.saa.2020.118895.

References

[1] G. Zhu, X. Zhu, Q. Fan, X. Wan, Spectrochim. Acta A Mol. Biomol. Spectrosc. 78 (2011) 1187–1195.
[2] R. Heald, A. Khodjakov, J. Cell Biol. 211 (2015) 1103.
[3] E. Karsenti, I. Vernos, Science 294 (2001) 543.
[4] K.S. Svoboda, C. F, B.J. Schnapp, S.M. Block, Nature 365 (1993) 721–727.
[5] L. Wordeman, Semin. Cell Dev. Biol. 21 (2010) 260–268.
[6] L.D. Barron, A.R. Gargaro, L. Hecht, P.L. Polavarapu, Spectrochim. Acta A: Mol. Spectrosc. 47 (1991) 1001–1016.
[7] L. Serrano, J. de la Torre, R.B. Maccioni, J. Avila, Proc. Natl. Acad. Sci. 81 (1984) 5989.
[8] E. S.M. Lakämper, Biophys. J. 89 (2005) 3223–3234.
[9] M. Sirajuddin, L.M. Rice, R.D. Vale, Nat. Cell Biol. 16 (2014) 335.
[10] L. N.L. Tajielyato, Y. Peng, J. Alper, E. Alexov, Scientific Reports 8 (2018) 13266.
[11] J. T.T.H. Luchko, M. Stepanova, J. Tuszynski, Biophys. J. 94 (2008) 1971–1982.
[12] P.W.T. Chelminiak, J. A, J.M. Dixon, Interdisciplinary Sciences: Computational Life Sciences 1 (2009) 108–112.
[13] A.L.T. Parker, W.S. Teo, J.A. McCarroll, M. Kavallaris, Int. J. Mol. Sci. 18 (7) (2017) 1434, https://doi.org/10.3390/ijms18071434.
[14] C.B. Janke, J. C, Nature Reviews Molecular Cell Biology (2011) 773–786.
[15] S.W. Westermann, K., Nature Reviews Molecular Cell Biology, (2003) 938–947.
[16] Y. Okada, N. Hirokawa, Proc. Natl. Acad. Sci. 97 (2000) 640.
[17] D.N. Reinemann, S.R. Norris, R. Ohi, M.J. Lang, Current Biology 28 (2018) 2356–2362.e2355.
[18] D.N. Reinemann, E.G. Sturgill, D.K. Das, M.S. Degen, Z. Vörös, W. Hwang, R. Ohi, M.J. Lang, Current Biology 27 (2017) 2810–2820.e2816.
[19] Z. Wang, M.P. Sheetz, Biophys. J. 78 (2000) 1955–1964.

[20] A.V. Gennerich, R. D, Curr. Opin. Cell Biol. 21 (2009) 59–67.
[21] G. Woehlke, A.K. Ruby, C.L. Hart, B. Ly, N. Hom-Booher, R.D. Vale, Cell 90 (1997) 207–216.
[22] A. Yildiz, M. Tomishige, R.D. Vale, P.R. Selvin, Science 303 (2004) 676.
[23] Y.E. Laurin, J.; Robert, C. H.; Prevost, C.; Sacquin-Mora, S, Biochemistry 56 (2017) 1746–1756.
[24] K.S.U. Thorn, J. A.; Vale, R. D., Journal of Cell Biology 151 (2000) 1093–1100.
[25] N. Peica, C. Lehene, N. Leopold, S. Schlücker, W. Kiefer, Spectrochim. Acta A Mol. Biomol. Spectrosc. 66 (2007) 604–615.
[26] A.K. Otter, G, Can. J. Chem. 66 (1988) 1814–1820.
[27] S.K. Sugiura, N.; Fujita, H.; Yamashita, H.; Momomura, S. I.; Chaen, S.; Omata, M.; Sugi, H., Circulation Research, 82 (1998) 1029–1034.
[28] K.P.P. Wall, M.; Armstrong, G.; Balsbaugh, J. L.; Verbeke, E.; Pearson, C. G.; Hough, L. E., ACS Chemical Biology 11 (2016) 2891–2990.
[29] H.L. Freedman, T.; Luduena, R. F.; Tuszynski, J. A., Proteins: Structure, Function, and Bioinformatics 79 (2011) 2968–2982.
[30] S.Z. Chakraborty, W, Biochemistry 54 (2015) 859–869.
[31] M.M. Panneerselvam, K.; Jayaraman, M.; Sridharan, U.; Jenardhanan, P.; Ramadas, K., Molecular Biosystems 9 (2013) 1470–1488.
[32] P. Echenique, G.A. Chass, eprint arXiv:0811.1271, (2008) arXiv:0811.1271.
[33] M. Elstner, K.J. Jalkanen, M. Knapp-Mohammady, T. Frauenheim, S. Suhai, Chem. Phys. 263 (2001) 203–219.
[34] K. Furić, V. Mohaček Grošev, M. Bonifačic, I. Štefanić, Raman Spectroscopic Study of H2O and D2O Water Solutions of Glycine, 1992.
[35] J.T.L. Navarrete, V. Hernández, F.J. Ramírez, Biopolymers 34 (1994) 1065–1077.
[36] M. Rožman, J. Am. Soc. Mass Spectrom. 18 (2007) 121–127.
[37] H.F. Shurvell, F.J. Bergin, J. Raman Spectrosc. 20 (1989) 163–168.
[38] W.R. Viviani, J.-L.; Csizmadia, I. G., Theoretica Chimica Acta, 85 (1993) 189–197.
[39] N. Kausar, T.J. Dines, B.Z. Chowdhry, B.D. Alexander, Phys. Chem. Chem. Phys. 11 (2009) 6389–6400.
[40] A.A. Bunaciu, H.Y. Aboul-Enein, V.D. Hoang, Appl. Spectrosc. Rev. 50 (2015) 377–386.
[41] J. De Gelder, K. De Gussem, P. Vandenabeele, L. Moens, J. Raman Spectrosc. 38 (2007) 1133–1147.
[42] A. Barth, Biochim. Biophys. Acta Bioenerg. 1767 (2007) 1073–1101.
[43] S. Bhunia, S.K. Srivastava, A. Materny, A.K. Ojha, J. Raman Spectrosc. 47 (2016) 1073–1085.
[44] C.F. Correia, P.O. Balaj, D. Scuderi, P. Maitre, G. Ohanessian, J. Am. Chem. Soc. 130 (2008) 3359–3370.
[45] N. Derbel, B. Hernández, F. Pflüger, J. Liquier, F. Geinguenaud, N. Jaïdane, Z. Ben Lakhdar, M. Ghomi, J. Phys. Chem. B 111 (2007) 1470–1477.
[46] S. Jaeqx, J. Oomens, A.M. Rijs, Phys. Chem. Chem. Phys. 15 (2013) 16341–16352.
[47] K.J. Jalkanen, S. Suhai, Chem. Phys. 208 (1996) 81–116.
[48] T.l.C. Jansen, A.G. Dijkstra, T.M. Watson, J.D. Hirst, J. Knoester, The Journal of Chemical Physics, 125 (2006) 044312.
[49] S. Kecel-Gunduz, B. Bicak, S. Celik, S. Akyuz, A.E. Ozel, J. Mol. Struct. 1137 (2017) 756–770.
[50] T. Kolev, M. Spiteller, B. Koleva, Amino Acids 38 (2010) 45–50.
[51] A.P. Mendham, T.J. Dines, M.J. Snowden, B.Z. Chowdhry, R. Withnall, J. Raman Spectrosc. 40 (2009) 1478–1497.
[52] J.T.L. Navarrete, V. Hernández, F.J. Ramírez, J. Mol. Struct. 348 (1995) 249–252.
[53] C.B. Silva, J.G. da Silva Filho, G.S. Pinheiro, A.M.R. Teixeira, F.F. de Sousa, P.T.C. Freire, Spectrochim. Acta A Mol. Biomol. Spectrosc. 229 (2020) 117899.
[54] E.G. Buchanan, W.H. James, S.H. Choi, L. Guo, S.H. Gellman, C.W. Müller, T.S. Zwier, J. Chem. Phys. 137 (2012), 094301.
[55] F. Eker, X. Cao, L. Nafie, R. Schweitzer-Stenner, J. Am. Chem. Soc. 124 (2002) 14330–14341.
[56] B.H. Pogostin, A. Malmendal, C.H. Londergan, K.S. Åkerfeldt, Molecules 24 (2019) 405.
[57] J. Ramos, V.L. Cruz, J. Mol. Model. 22 (2016) 273.
[58] K. Rybka, S.E. Toal, D.J. Verbaro, D. Mathieu, H. Schwalbe, R. Schweitzer-Stenner, Proteins Struct. Funct. Bioinforma. 81 (2013) 968–983.
[59] B. Sjöberg, S. Foley, B. Cardey, M. Enescu, Spectrochim. Acta A Mol. Biomol. Spectrosc. 128 (2014) 300–311.
[60] H. Valdes, V. Spiwok, J. Rezac, D. Reha, A.G. Abo-Riziq, M.S. de Vries, P. Hobza, Chem. Eur. J. 14 (2008) 4886–4898.
[61] P. Bour, J. Kubelka, T.A. Keiderling, Biopolymers 65 (2002) 45–59.
[62] S. Habka, W.Y. Sohn, V. Vaquero-Vara, M. Géléoc, B. Tardivel, V. Brenner, E. Gloaguen, M. Mons, Phys. Chem. Chem. Phys. 20 (2018) 3411–3423.
[63] S.R. Huang, Y. Liu, F. Tureček, Phys. Chem. Chem. Phys. 21 (2019) 2046–2056.
[64] B. Martial, T. Lefèvre, M. Auger, Biophys. Rev. 10 (2018) 1133–1149.
[65] D.A.T. Pires, L.M.R. Arake, L.P. Silva, A. Lopez-Castillo, M.V. Prates, C.J. Nascimento, C. Bloch, Peptides 106 (2018) 37–44.
[66] K. Furić, V. Mohaček Grošev, M. Bonifačic, I. Štefanić, J. Mol. Struct. 267 (1992) 39–44.
[67] M. Paulite, C. Blum, T. Schmid, L. Opilik, K. Eyer, G.C. Walker, R. Zenobi, ACS Nano 7 (2013) 911–920.
[68] E. Podstawka, G. Niaura, L.M. Proniewicz, J. Phys. Chem. B 114 (2010) 1010–1029.
[69] S. Stewart, P.M. Fredericks, Spectrochim. Acta A Mol. Biomol. Spectrosc. 55 (1999) 1615–1640.
[70] X. Yang, C. Gu, F. Qian, Y. Li, J.Z. Zhang, Anal. Chem. 83 (2011) 5888–5894.
[71] J.S. Suh, M. Moskovits, J. Am. Chem. Soc. 108 (1986) 4711–4718.
[72] J.T. Kelly, A.K. McClellan, L.V. Joe, A.M. Wright, L.T. Lloyd, G.S. Tschumper, N.I. Hammer, Chemphyschem 17 (2016) 2782–2786.
[73] C.A. Jiménez-Hoyos, B.G. Janesko, G.E. Scuseria, Phys. Chem. Chem. Phys. 10 (2008) 6621–6629.
[74] A. Parameswari, S. Premkumar, R. Premkumar, A. Milton Franklin Benial, J. Mol. Struct. 1116 (2016) 180–187.
[75] P.S. Walsh, J.C. Dean, C. McBurney, H. Kang, S.H. Gellman, T.S. Zwier, Phys. Chem. Chem. Phys. 18 (2016) 11306–11322.
[76] M.J. Frisch, G.W. Trucks, H.B. Schlegel, G.E. Scuseria, M.A. Robb, J.R. Cheeseman, G. Scalmani, V. Barone, G.A. Petersson, H. Nakatsuji, X. Li, M. Caricato, A.V. Marenich, J. Bloino, B.G. Janesko, R. Gomperts, B. Mennucci, H.P. Hratchian, J.V. Ortiz, A.F. Izmaylov, J.L. Sonnenberg, Williams, F. Ding, F. Lipparini, F. Egidi, J. Goings, B. Peng, A. Petrone, T. Henderson, D. Ranasinghe, V.G. Zakrzewski, J. Gao, N. Rega, G. Zheng, W. Liang, M. Hada, M. Ehara, K. Toyota, R. Fukuda, J. Hasegawa, M. Ishida, T. Nakajima, Y. Honda, O. Kitao, H. Nakai, T. Vreven, K. Throssell, J.A. Montgomery Jr., J.E. Peralta, F. Ogliaro, M.J. Bearpark, J.J. Heyd, E.N. Brothers, K.N. Kudin, V.N. Staroverov, T.A. Keith, R. Kobayashi, J. Normand, K. Raghavachari, A.P. Rendell, J.C. Burant, S.S. Iyengar, J. Tomasi, M. Cossi, J.M. Millam, M. Klene, C. Adamo, R. Cammi, J.W. Ochterski, R.L. Martin, K. Morokuma, O. Farkas, J.B. Foresman, D.J. Fox, Gaussian 16 Rev. B.01, in, Wallingford, CT, 2016.
[77] R.B. Krishnan, J. S.; Seeger, R.; Pople, J. A., Journal of Chemical Physics, 72 (1980) 650–654.
[78] A.D. Becke, J. Chem. Phys. 98 (1993) 5648–5652.
[79] C. Lee, W. Yang, R.G. Parr, Phys. Rev. B 37 (1988) 785–789.
[80] M.P. Andersson, P. Uvdal, J. Phys. Chem. A 109 (2005) 2937–2941.